Available online at www.sciencedirect.com

SciVerse ScienceDirect

Ceramics International 39 (2013) 8199–8206

CERAMICS INTERNATIONAL

www.elsevier.com/locate/ceramint

Mechanical behavior of electrospun Nylon66 fibers reinforced with pristine and treated multi-walled carbon nanotube fillers

Kyung Soo Jeon[a], R. Nirmala[a,*], R. Navamathavan[b], Hak Yong Kim[a,*]

[a]Department of Organic Materials and Fiber Engineering, Chonbuk National University, Jeonju, 561-756, South Korea
[b]School of Advanced Materials Engineering, Chonbuk National University, Jeonju, 561-756, South Korea

Received 25 February 2013; received in revised form 1 April 2013; accepted 1 April 2013
Available online 16 April 2013

Abstract

In this paper, we report the preparation and characterization of electrospun Nylon66 composite nanofibers incorporated with treated and untreated multi-walled carbon nanotube (MWCNT). In order to improve the mechanical properties, we added surface treated MWCNT (TMWCNT) in to the Nylon66 composite nanofibers. The resultant composite nanofibers were characterized by using scanning electron microscopy, energy dispersive X-ray analysis, X-ray diffraction, Fourier transform infrared spectroscopy, Raman spectroscopy, UV–vis spectroscopy and thermogravimetric analysis. The morphological analysis revealed that very clear arrangement of ultra-fine mesh-like nanofibers strongly bound with the main fibers. The mechanical properties of the composite nanofibers such as Young's modulus, tensile strength and elongation-at-break were improved than pristine Nylon66 nanofibers. The addition of a relatively small amount (0.5 wt%) of TMWCNT in to the electrospun Nylon66 composite nanofibers significantly enhanced the mechanical properties. The improved mechanical property of the composite nanofibers can be explained based on thermal studies.

Keywords: Nylon66; Multiwalled carbon nanotube; Nanofibers; Mechanical strength

1. Introduction

Recent advances in electrospinning technique have shown that the electrospun polymer nanofibers possess attractive attributes such as enhanced strength and modulus compared to micrometer-scale fibers [1–5]. These features can be of significant importance, particularly when the nanofibers are intended for miniaturized, load-bearing applications [6]. A few investigators reported their findings on improving the mechanical properties of the electrospun nanofibers [7,8]. Recently, it was found that the tensile strength and modulus of the fibers depend greatly on the fiber size. For example, reducing the fiber diameter leads to strengthening effects [1,2]. However, handling nanofibers that are just a few tens of nanometers in size and characterizing their tensile modulus has been fraught with difficulties. Alternatively, the mechanical integrity of the fibers can be significantly improved by incorporating high strength and high aspect ratio nano-fillers to obtain novel composite nanofibers such that they possess remarkably superior mechanical strength [7,8]. Furthermore, it is demonstrated that electrospinning polymer solutions dispersed with filler materials is a unique technique to efficiently disperse, align and orientate the particles [7–9]. The fillers are self-assembled and carried by the spun fibers and possess improved strength and stiffness than the filler-dispersed composites that are obtained using the conventional extrusion techniques [1,7,8].

Polymer/nanoparticle interfaces play an important role in new applications involving hybrid materials, where nanoparticles are added to a polymer to alter its structural and mechanical properties without affecting the main chemical features of the supporting matrix [10]. Among them, carbon nanotubes (CNTs) have been considered as a nonpareil candidate for polymer reinforcement owing to their extraordinary mechanical, electrical, and thermal properties, as well as their high aspect ratio. The properties of polymer/CNTs composites have been intensively investigated by many researchers [11–13]. Also, many methods have been used to fabricate CNT/polymer composites with high mechanical reinforcement over the past decade [14,15]. CNTs have often played an accelerating role in polymer crystallization as a nucleating agent in polymer matrix [16–19].

*Corresponding authors. Tel.: 82 63 270 2351; fax: 82 63 270 4249.
E-mail addresses: rnn12@yahoo.com (R. Nirmala), khy@jbnu.ac.kr (H.Y. Kim).

0272-8842/$ - see front matter © 2013 Elsevier Ltd and Techna Group S.r.l. All rights reserved.
http://dx.doi.org/10.1016/j.ceramint.2013.04.003

Due to the small diameter and extremely hydrophobic surface property of CNTs, however, it is difficult to achieve homogenous dispersion of CNTs within a polymeric material matrix. The most relevant issues are to disperse CNTs well in polymer matrix and to create a strong interfacial binding between the polymer matrix and the CNTs [20,21].

On the basis of reaction chemistry, two approaches have been explored to achieve covalent functionalization of CNT: the first approach involves directly attaching functional groups to the graphitic surface and in the second approach, the functional groups are linked to the CNT-bound carboxylic acids, which are created during CNT synthesis or post treatment of CNTs for purification purpose. These carboxylic acids are considered as the defect sites on the CNT surface and the method is also known as the defect chemistry method [22]. The advantage of the chemical functionalization method is that the functional groups are covalently linked to the CNT surface; the linkage is permanent and mechanically stable. However, reaction with the graphitic sheets also results in breaking the sp2 conformation of the carbon atoms. Conjugation of the CNT wall is therefore disrupted and it has been observed that, compared with the pristine tubes, electrical and mechanical properties of the chemically functionalized CNTs decreased dramatically [22–24]. The non-covalent methods to functionalize CNTs involve using soft matter such as surfactants, oligomers, biomolecules and polymers to wrap CNTs, to enhance their solubility [22,25,26]. The advantage of the non-covalent method is that the integrity of CNT structure is not disrupted and the properties of the CNTs are therefore retained. However, the non-covalent interaction between the wrapping molecules and the CNTs is not as strong as the covalent bonds formed in the chemical functionalization processes [22].

Nylon66 is an important engineering thermoplastics which has been used for numerous technological applications due to its favorable properties such as chemical and mechanical resistance, attrition resistance, high tensile and melting point [27]. Recent usage of Nylon66 and polyamides in general has focused on their use in automotive under-the-hood applications for the driving force being greater fuel economy and weight reductions coupled with the critical requirements of high temperature usage and resistance to thermal degradation.

In the present paper, we describe the changes in the tensile, flexural and impact properties of Nylon66 with multi-walled carbon nanotube (MWCNT). We prepared Nylon66 nanofibers containing MWCNT and treated multi-walled carbon nanotube (TMWCNT) by using electrospinning for studying the effect of composite by thermal and mechanical analysis. The resultant composite nanofibers were characterized by scanning electron microscopy (SEM), energy dispersive X-ray analysis (EDX), X-ray diffraction (XRD), Fourier transform (FT-IR), UV–vis, Raman spectroscopy and thermogravimetric analysis (TGA).

2. Experimental

2.1. Materials

Nylon66 was supplied by Sigma Aldrich. Formic acid (99%), sulfuric acid (H_2SO_4) and nitric acid (HNO_3) were obtained from Samchun Chemicals, South Korea. MWCNT with 95% purity and diameter < 10 nm and length < 20 μm were purchased from Nanosolution Co., Ltd. Korea. All the above chemical reagents used were of analytical grade and used without further purification.

2.2. Preparation of treated MWCNT

To improve the mechanical properties of the MWCNT, we treated MWCNT with surface modifications. We performed a 3:1 (v/v) mixture of concentrated H_2SO_4/HNO_3 (100 ml) to treat MWCNTs (200 mg), with sonication at 60 °C for 5 h. After acid treatment, MWCNTs were washed using deionized water and ethanol. The mixture was filtered until the pH value of 7 was reached and then dried at 80 °C for 24 h. The resulting material is labeled as TMWCNT. The acid treated MWCNTs with a higher concentration of carboxylic acid (–COOH) groups can form a stronger MWCNT–Nylon66 interfacial interaction, which consequently improves the mechanical properties.

2.3. Polymer solution preparation

Three kinds of spin dopes were prepared as the following: (1) 10 wt% of Nylon66 solution was prepared in the formic acid solvent, (2) 10 wt% of Nylon66 with 0.5 wt% of MWCNT and (3) 10 wt% Nylon66 with 0.5 wt% of TMWCNT were prepared to obtain Nylon66, Nylon66/MWCNT and Nylon66/TMWCNT nanofibers. Before the electrospinning process, the prepared solutions were stirred well to make uniform mixture. We have used the optimized condition to prepared composite nanofibers. The dispersion of the MWCNTs (above 0.5 wt% loading) were not very good in the Nylon66 matrix as the MWCNT (non-polar nature) were non-functionalized and so the inherent incompatibility with the polar Nylon66 matrix.

2.4. Electrospinning

The polymer solution was transferred into a 5 ml syringe fitted with a metallic needle of 0.4 mm of inner diameter. The syringe was fixed horizontally on the syringe stand and the positive electrode of the high voltage power supply (CPS-60K02vl, Chungpa EMT Co., South Korea), capable of generating voltages up to 60 kV, was clamped to the metal needle tip. The applied voltage was fixed at 18 kV and the tip-to-collector distance was kept at 15 cm. All the experiments were conducted at room temperature. These experimental parameters were chosen from an optimization of a series experiments. The developed nanofiber mats were collected on the rotating drum covered with the collecting blue paper.

2.5. Characterizations

The morphology of the Nylon66, Nylon66/MWCNT and Nylon66/TMWCNT composite nanofibers were observed by using SEM (Hitachi S-7400, Hitachi, Japan). Elemental composition analyses of these composite nanofibers were carried out by using a field-emission SEM equipped with an EDX spectrometer. Structural characterization was carried out by XRD in a

Rigaku X-ray diffractometer operated with Cu Kα radiation ($\lambda = 1.540$ Å). The bonding configurations of the samples were characterized by means of FT-IR spectroscopy and Raman spectroscopy. TGA (Perkin-Elmer, USA) was carried out for the composite nanofibers under nitrogen ambient with a flow rate of 20 mL/min. The samples were heated from 30 to 800 °C at a rate of 10 °C/min. Differential scanning calorimetry (DSC, Perkin-Elmer, USA) characterizations were performed for the electrospun nanofibers. The UV–vis spectra were measured in the range of 200–800 nm by using a UV–vis spectrometer (Lambda 900, Perkin-Elmer, USA). Mechanical properties were measured with a universal testing machine (AG-5000 G, Shimadzu, Japan), under a head speed of 10 mm/min at room temperature. The samples were prepared in the form of standard dumbbell shapes according to ASTM Standard D638 by using die cutting of the electrospun mats and tested in the machine direction.

3. Results and discussion

Fig. 1(a)–(c) shows the SEM images of the pristine Nylon66, Nylon66/MWCNT and Nylon66/TMWCNT composite nanofibers. As shown in these figures, the pristine and composite nanofibers were observed to be smooth and bead-free nature. Also, it was observed that a very clear arrangement of ultra-fine mesh-like nanofibers strongly bound within the main nanofibers.

Fig. 2(a)–(c) shows the FESEM images and FESEM EDX spectra of pristine Nylon66, Nylon66/MWCNT and Nylon66/TMWCNT composite nanofibers. Ultra-fine nanofiberes were observed in the Nylon66 and Nylon66/MWCNT and Nylon66/TMWCNT composite mats which results in a large surface to volume ratio. The nanofiber diameter was in the range of 200–300 nm, whereas the diameter of ultra-fine nanofibers formed in between the main nanofibers was in the range about 10–50 nm. The Nylon66 bearing reactive functional groups that may yield reactions of chemical exchange when they are mixed with solvent (formic acid) resulted in a poly-electrolytic behavior of the solution [28,29] forming ultra-fine nanofibers. As shown in EDX spectra, no other element impurity is detected indicating that the final product is free of impurity. The successful incorporation of MWCNT in the Nylon66 composite nanofibers was confirmed by the EDX spectra.

Detailed XRD analysis of pristine and composites of MWCNT, TMWCNT, Nylon66, Nylon66/MWCNT and Nylon66/TMWCNT samples were performed to study the comparative structural characterization. The XRD diffractograms of these pristine and composite materials are shown in Fig. 3. As indicated, three distinct diffraction peaks were appeared at 2θ value of 15.45, 25.1 and 41.99° corresponding to the (100) and (010) and (110) planes of MWCNT, respectively. On the other hand, the treated MWCNT showed only one broad peak at 24.25° corresponding to (010) plane. The other two diffraction peaks were disappeared due to the acid treatment of MWCNT. In the case of Nylon66 nanofibers, two prominent diffraction peaks at 15.9 and 22.5° corresponding to (100) and (010) planes are indexed and for the Nylon66/MWCNT composite nanofibers the diffraction peaks at the 2θ value of 20.45° and 23.48° are assigned to the (100) and (010) planes. On the other hand, the diffraction peak of Nylon66/TMWCNT showed a broad peak 15–22° centered at 18° was observed. This broad diffraction peak indicates that the Nylon66/TMWCNT composite nanofibers were of amorphous nature. The diffraction peaks of electrospun fibers were

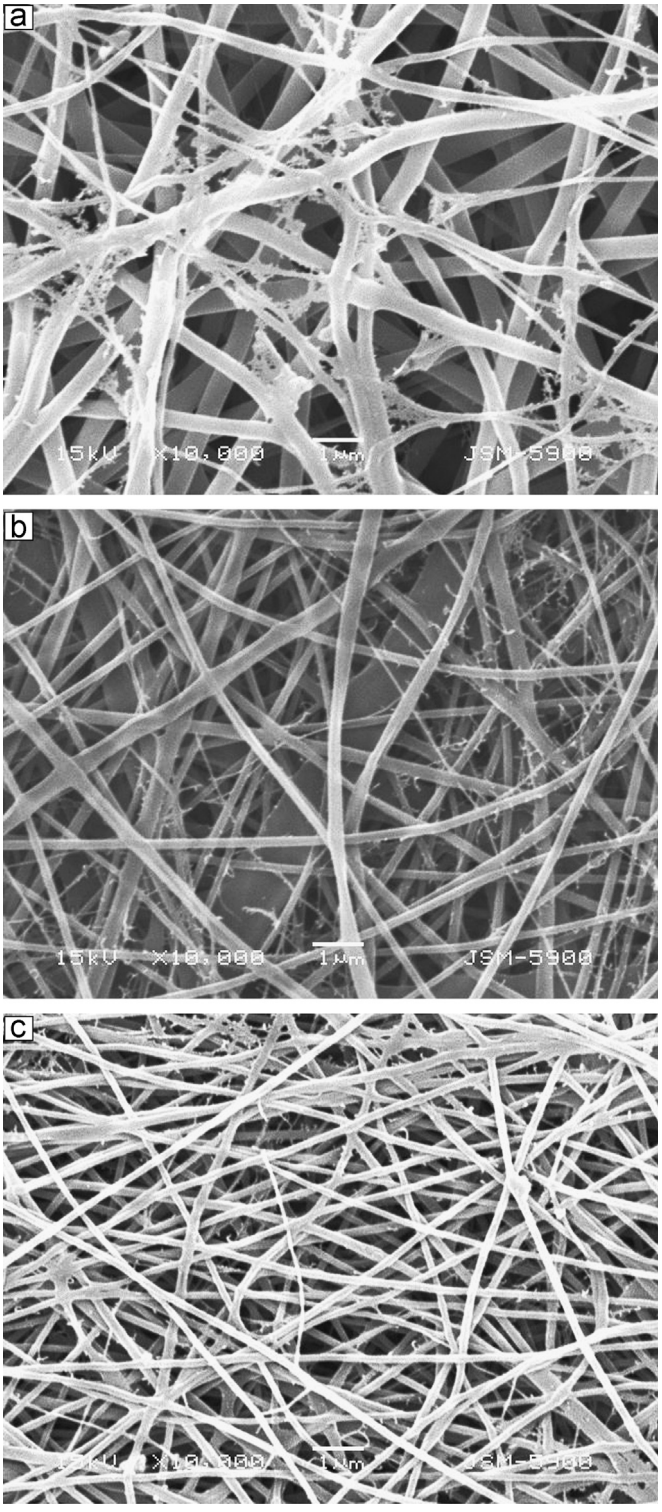

Fig. 1. SEM images of (a) Nylon66, (b) Nylon66/MWCNT and (c) Nylon66/TMWCNT nanofibers.

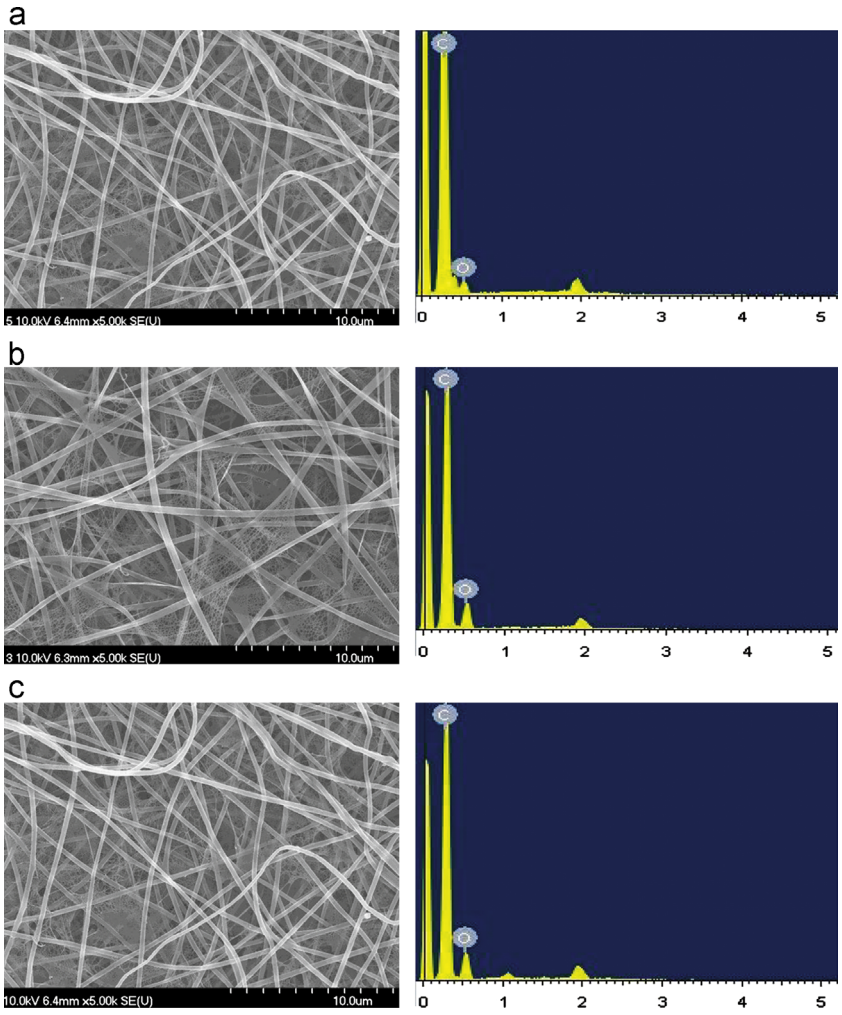

Fig. 2. FESEM images and FESEM-EDX spectra of (a) Nylon66, (b) Nylon66/MWCNT and (c) Nylon66/TMWCNT nanofibers.

reduced because the macromolecular chain was loosely arranged due to the rapid evaporation of solvent during the electrospinning process [30]. The XRD results indicated that electrospun composite nanofibers possessed a lower degree of crystallinity than pristine Nylon66 nanofibers. No significant diffraction peaks of any other phases or impurities can be detected in the XRD patterns, which indicate the successful formation of Nylon66, Nylon66/MWCNT and Nylon66/TMWCNT composite nanofibers.

The structural configurations of MWCNT, TMWCNT, Nylon66, Nylon66/MWCNT and Nylon66/TMWCNT composite nanofibers were characterized by using FT-IR spectroscopy. Fig. 4 illustrates the FT-IR spectra of the interaction between pristine and composite materials. As shown in the FT-IR spectrum of MWCNT, the peaks at 1634 and 1795 cm^{-1} correspond to C=O and C–O stretching modes. The two weak peaks at 2917 and 2847 cm^{-1} correspond to the –CH stretching mode. A broad peak corresponding to strong transmittance from 3200 to 3400 cm^{-1} can be ascribed to –OH stretching vibration in –COOH group [31]. On the other hand, a significant structural change was observed in the case of treated MWCNT. The intensity of C=O, C–O stretching modes and –OH related bonding were significantly reduced for the TMWCNT. After acid treatment MWCNT show a reduced IR peak at 1634 and 1795 cm^{-1} indicating that the decreasing of C=O stretching vibration of carboxylic acid groups [32,33]. A strong and sharp peaks at 1631 and 1707 cm^{-1} are ascribed to C=O stretching vibration due to the formation of amide linkage; and another peak at 1184 cm^{-1} corresponds to C–N stretching of amide group for the Nylon66 nanofibers was also assigned. The two weak peaks at 2917 and 2847 cm^{-1} correspond to the –CH stretching mode. On the other hand, the C=O stretching vibration peaks significantly increased for the Nylon66/MWCNT and Nylon/TMWCNT composite nanofibers. Additional peak at 725 cm^{-1} corresponds to the bending vibration of C=O group was also appeared for the composite nanofibers. It is importantly noted that the drastic reduction of the broad peak around 3200–3400 cm^{-1} due to –COOH functional groups which gets converted into polyimide. The peak around 1550 cm^{-1} is attributed to the C=C stretching mode associated with sidewall attachment for the acid treated MWCNT. Therefore, the incorporation of TMWCNT might perturb the intermolecular interaction of hydrogen bonding between polyamide molecules, but not transform the crystal phase structure of Nylon66. These FT-IR data clearly confirms the successful incorporation of MWCNT and TMWCNT into Nylon66 composite nanofibers.

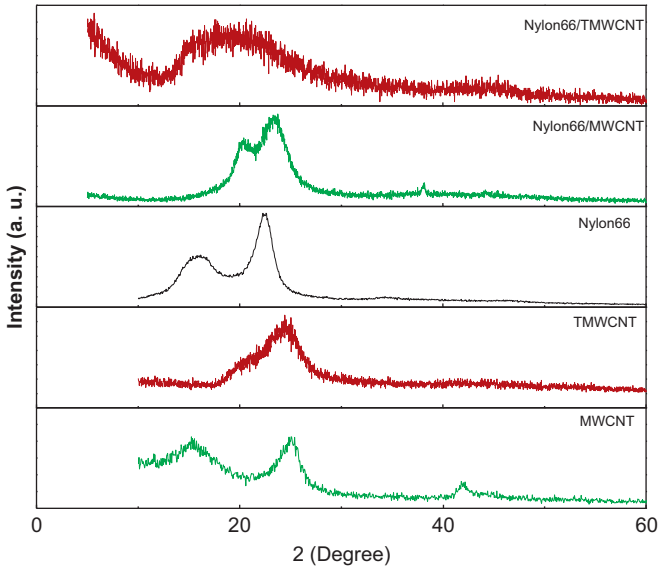

Fig. 3. XRD patterns of MWCNT, TMWCNT, Nylon66, Nylon66/MWCNT and Nylon66/TMWCNT nanofibers.

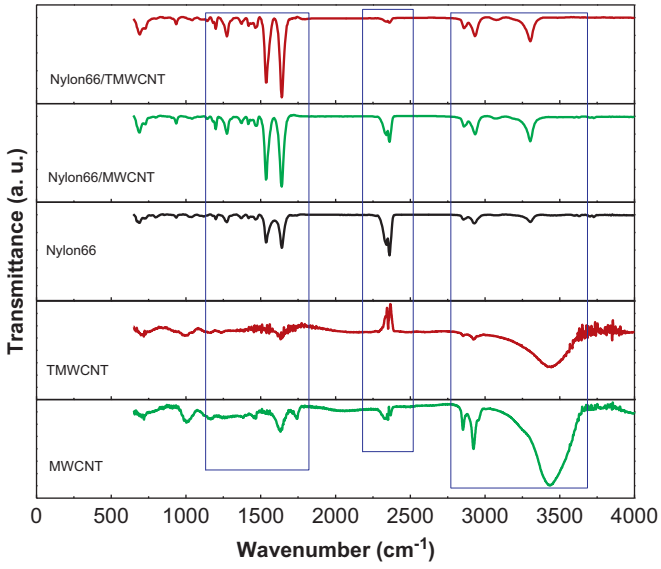

Fig. 4. FT-IR spectra of MWCNT, TMWCNT, Nylon66, Nylon66/MWCNT and Nylon66/TMWCNT nanofibers.

Fig. 5 shows the Raman spectra of the MWCNT, TMWCNT, Nylon66, Nylon66/MWCNT and Nylon66/TMWCNT. The MWCNT functionalization was further confirmed by observing the structural and morphological changes in pristine and composite materials using Raman spectroscopy. The covalent attachment of functional entities and the hybridization of sidewall of C atoms had a significant effect on the intensity ratio of the Raman bands. Raman analyses have been demonstrated in two characteristic peaks at 1330 cm^{-1} (D band) and 1585 cm^{-1} (G band). The D band arises from the generation of sp3 C atoms as defects in the sp2 carbon lattice, whereas the G band indicates the presence of ordered sp2 hybridization [34,35]. The intensity ratio between the D and the G bands (ID/IG) indicates the extent of functionalization. The treated MWCNTs exhibited a pronounced increase in the ID/IG ratio when compared to the

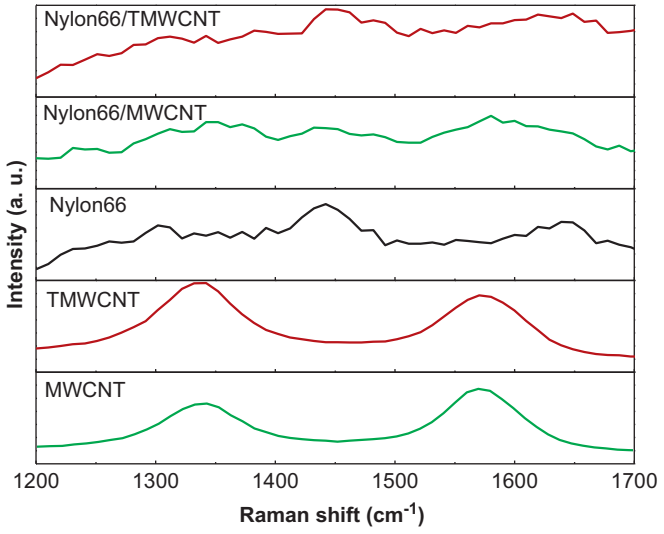

Fig. 5. Raman spectra of MWCNT, TMWCNT, Nylon66, Nylon66/MWCNT and Nylon66/TMWCNT nanofibers.

pristine MWCNTs, which was indicative of covalent sidewall attachment of the functional groups. The components MWCNT composite nanofibers were semi-quantitatively evaluated using Raman spectroscopy. As shown in Fig. 5, the Raman spectra of MWCNT and TMWCNT, Nylon 66 and the composite nanofibers, the G band at 1580 cm^{-1} did not overlap with any bands in the Nylon66 spectrum and therefore can be used as the reference for the semi-quantitative comparison of MWCNT composition with the composite nanofibers. The band at 1640 cm^{-1} is due to C–O stretch of amide groups in Nylon66 [36]. As we incorporate MWCNT and TMWCNT in to Nylon66, the intensity of D and G bands became much reduced than that of pristine materials. Raman spectra provide further evidence of –COOH functionalization of the MWCNT with electrospun Nylon66 composite nanofibers. Also, the D band of Nylon66/MWCNT is shifted upward from 1330 to 1370 cm^{-1} as compared to pristine MWCNT. The disorder nature of Nylon66/MWCNT and Nylon66/TMWCNT composite nanofibers was attributed to sp3-hybrized carbon in the MWCNT walls and amorphous carbon. For the acid treated MWCNT, the –COOH groups can act as electron acceptors which are covalently attached to the nanotube walls. The FT-IR and Raman measurements effectively show that MWCNT with –COOH functional groups was produced during the acid treatment and subsequently converted to functionalize MWCNT as evidenced by the amide group. This result is in good agreement with the FT-IR data.

Fig. 6 shows the TGA analyses of Nylon66, Nylon66/MWCNT and Nylon66/TMWCNT composite nanofibers. Typical TG curves and the corresponding derivative thermogravimetric (DTG) curves obtained at a heating rate of 10 °C/min for Nylon66, Nylon66/MWCNT and Nylon66/TMWCNT composite nanofibers are shown in Fig. 6(a) and (b). The small humps at around 300–350 °C in the DTG curves are due to the loss of moisture in Nylon66/MWCNT sample. The onset of decomposition of pristine and composite nanofibers was found to be in the range of 300–420 °C, as shown in Fig. 6(a). The Nylon66/MWCNT nanofibers

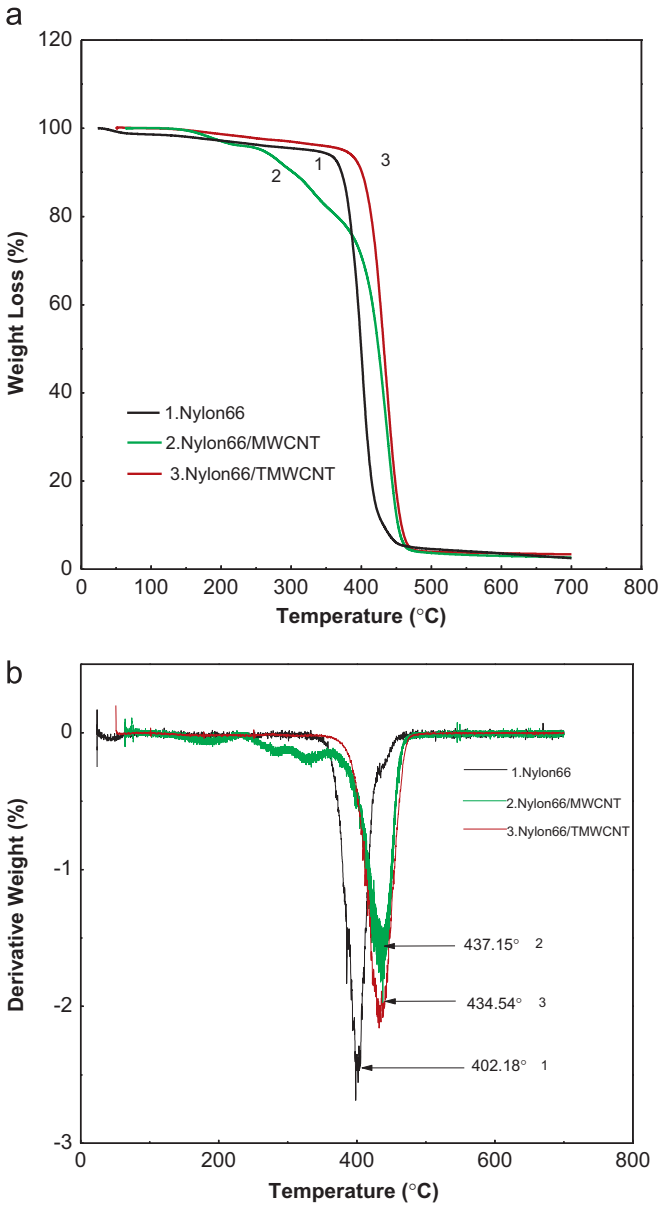

Fig. 6. (a) Thermogravimetric analysis of Nylon66, Nylon66/MWCNT and Nylon66/TMWCNT nanofibers and (b) derivative thermogravimetric curves of Nylon66, Nylon66/MWCNT and Nylon66/TMWCNT nanofibers.

showed reduced onset decomposition temperature and multi-step degradation than that of the pristine and Nylon66/TMWCNT composite nanofibers. This result is attributed to the low molecular weight oligomers present in the nanofibers. On the other hand, the functionalized Nylon66/TMWCNT nanofibers exhibited single-step degradation with increased onset decomposition temperature. As expected, the residual weight slightly increases with the addition of MWCNT in the Nylon66 nanofibers. As shown in Fig. 6(b), the derivative TGA curves correspond to Nylon66/MWCNT showed multi-stage degradation peaks.

DSC was employed to evaluate the effect of MWCNTs on the phase transition behavior of pristine and composite nanofibers. Fig. 7 shows the DSC of Nylon66, Nylon66/MWCNT and Nylon66/TMWCNT composite nanofibers. For the pristine Nylon66 nanofibers (Fig. 7a), the glass transition

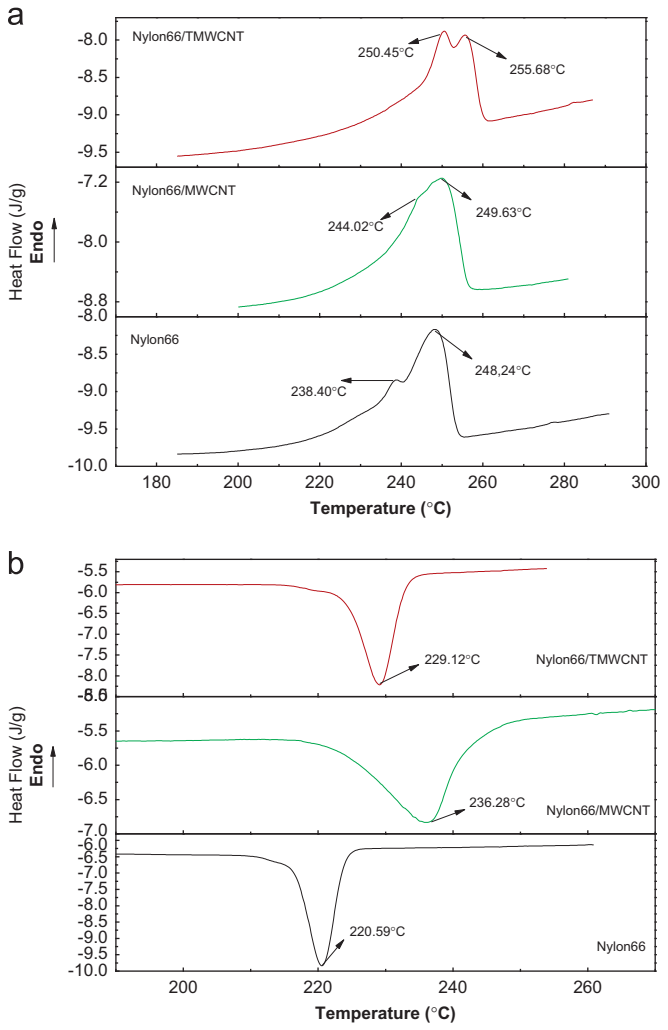

Fig. 7. DSC scans of Nylon66, Nylon66/MWCNT and Nylon66/TMWCNT nanofibers. Heating (a) and cooling (b) rates of 10 °C/min.

temperatures were appeared at 238 and 248 °C. The behavior of multi-melting peaks in Nylon66 has been observed and discussed before for both pristine Nylon66 [37,38] and Nylon66 composites [39–43]. Bell et al. reported that Nylon66 exhibited two melting peaks, which might appear singly or together depending on the annealing and drawing treatment [44]. The glass transition temperature was found to be increased with the incorporation of MWCNT and TMWCNT.

The crystallization temperature of pristine Nylon66 nanofibers appeared at 232.4 °C (Fig. 7b). The crystallization temperatures of Nylon66/MWCNT and Nylon66/TMWCNT composite nanofibers were of 235.6 and 230.7 °C, respectively. In addition, the crystallization temperatures were slightly shifted toward lower and higher temperature for the TMWCNT and MWCNT incorporated composite nanofibers, respectively. The DSC results indicates that the pristine Nylon66 nanofibers in the relaxed state, good crystallization occurs from melting and annealing without any constraint, and that drawing of pristine Nylon66 nanofibers leads to well-developed crystallization with molecular orientation. However, when the MWCNT are incorporated, the Nylon66 nanofibers

well mixed with MWCNT are difficult to crystallize perfectly under highly stressed conditions such as drawing, because the presence of well-dispersed MWCNT interrupts the chain mobility of the Nylon66 molecules, which depresses crystallization. Therefore, these results indicate that the crystallization of composite nanofibers is largely affected by the stressed state of nanofibers and MWCNT dispersion in polymer matrix, as well as by the mechanical properties of the composite fibers.

Fig. 8 shows the strain–stress curves of the Nylon66, Nylon66/MWCNT and Nylon66/TMWCNT nanofibers. The mechanical properties of the composite nanofibers such as Young's modulus, tensile strength and elongation-at-break appeared to be increased than those of the pristine Nylon66 nanofibers (Table 1). Generally, MWCNT-based polymer composites have better mechanical properties than pristine polymers owing to the reinforcing effect of MWCNT. Although the Young's modulus of the Nylon66/MWCNT nanofibers was observed to be highest (46 MPa) among all the samples, however, in this study, the electrospun Nylon66/MWCNT composite nanofibers showed very poor breaking stress (28%) than that of pristine Nylon66 nanofibers (61%). On the other hand, the treated and functionalized Nylon66/TMWCNT composite nanofibers showed higher breaking stress (82%) than the pristine Nylon66 nanofibers at the same draw ratio. Therefore, we believe that the functionalized MWCNT can improve the overall mechanical properties of the Nylon66/TMWCNT nanofibers, which is advantageous as per the applications are concerned. In many CNT/polymer composites, well-dispersed CNT have induced polymer crystallization and thus improve the breaking stress of the composites [23–25]. In another study, it was reported that the filling of treated-MWCNTs into the epoxy matrix would result in the descent of bending property of the epoxy composites [36]. Therefore, it is important to understand why the Nylon66/MWCNT and Nylon66/TMWCNT composite nanofibers showed different breaking stress at the same draw ratio when compared to pristine Nylon66 nanofibers, which differs from MWCNT composites in the bulk state.

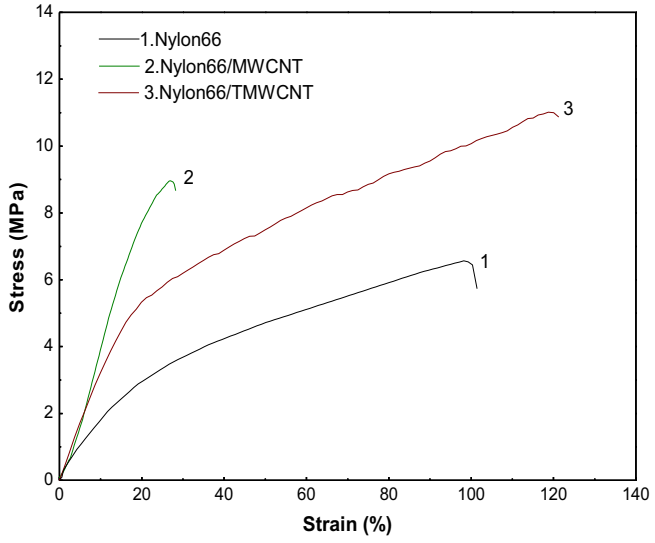

Fig. 8. Tensile test curves of Nylon66, Nylon66/MWCNT and Nylon66/TMWCNT nanofibers.

Table 1
Mechanical properties of the electrospun pristine Nylon66, Nylon66/MWCNT and Nylon66/TMWCNT nanofibers.

Sample	Young's modulus (MPa)	Tensile strength (MPa)	Elongation at break (%)
Nylon66	29.05 ± 3.2	6.58 ± 0.8	61 ± 1.2
Nylon66/MWCNT	46.7 ± 4.1	8.97 ± 1.3	28.5 ± 0.6
Nylon66/TMWCNT	36.58 ± 2.7	11.39 ± 1.1	82.2 ± 1.8

Nylon66 in the presence of formic acid under goes a chain breaking reaction and can produce the zwitter ions which results in the formation of ultra-fine nanofibers. The pristine MWCNT when mixed in to the Nylon66 solution, the amine functionalization of the MWCNT takes place and so the functionalized MWCNT form again the bond between the NH CO which results in the aggregation of the MWCNT in the solution. Whereas the –COOH functionalized MWCNT when added in to the solution they react with the zwitter ion (the zwitter ion act as the surfactant) and COOH+NH_2 forming the amide bond that helps in the free dispersion of the MWCNT. That's why the –COOH functionalized MWCNT incorporated in to Nylon66 composite nanofiber mats exhibited a good mechanical properties compared to that of other samples.

4. Conclusions

We have successfully obtained MWCNT and TMWCNT incorporated Nylon66 composite nanofibers by using electrospinning technique. The Nylon66/TMWCNT composite nanofibers showed good mechanical property. The resultant composite nanofibers were characterized by using SEM, EDX, XRD, FT-IR, Raman, TGA, and DSC analyses. Dispersion of acid-treated MWCNTs in Nylon66 composite nanofibers was enhanced owing to the increased interaction between Nylon66 molecules and functionalized groups present on the surfaces of TMWCNT. The mechanical properties of composite nanofibers were differed with the incorporation of pure and functionalized MWCNT. These findings indicated that disturbance in crystallization and the molecular orientation of Nylon66 is caused by the highly constrained state of MWCNT-incorporated in the composite nanofibers. However, the enhanced the mechanical property Nylon66/TMWCNT composite nanofibers were attributed to the crystallization of Nylon66 molecules under stressed and relaxed states and treated MWCNT dispersion in the polymer matrix.

Acknowledgments

This research was financially supported by the Ministry of Education, Science Technology (MEST) and National Research Foundation of Korea (NRF) through the Human Resource Training project for regional Innovation (Project number 2012H1B8A2025931). The research was also

supported by the "Leaders in Industry–University Cooperation" Project, which is funded by the Ministry of Education, Science & Technology (MEST) and the National Research Foundation of Korea (NRF) (2012-C-0043-010120).

References

[1] S.C. Wong, A. Baji, S.W. Leng, Effect of fiber diameter on tensile properties of electrospun poly(ε-caprolactone), Polymer 21 (2008) 4713–4722.
[2] A. Arinstein, M. Burman, O. Gendelman, E. Zussman, Effect of supramolecular structure on polymer nanofiber elasticity, Nature Nanotechnology 2 (2007) 59–62.
[3] E.P.S. Tan, S.Y. Ng, C.T. Lim, Tensile testing of single ultrafine polymeric fiber, Biomaterials 26 (2005) 1453–1456.
[4] E. Zussman, M. Burman, A.L. Yarin, R. Khalfin, Y. Cohen, Tensile deformation of electrospun nylon-6, 6 nanofibers, Journal of Polymer Science Part B: Polymer Physics 44 (2006) 1482–1489.
[5] R. Nirmala, J.W. Jeong, R. Navamathavan, H.Y. Kim, Synthesis and electrical properties of TiO_2 nanoparticles embedded in polyamide-6 nanofibers via electrospinning, Nano-Micro Letters 3 (2011) 56–61.
[6] F.K. Ko, S. Sukigara, M. Gandhi, J. Ayutsede, Electrospun carbon nanotube reinforced silk fibers, US patent no. 0082197; 2007.
[7] Y. Dror, W. Salalha, R.L. Khalfin, Y. Cohen, A.L. Yarin, E. Zussman, Carbon nanotubes embedded in oriented polymer nanofibers by electrospinning, Langmuir 19 (2003) 7012–7020.
[8] W. Salalha, Y. Dror, R.L. Khalfin, Y. Cohen, A.L. Yarin, E. Zussman, Single-walled carbon nanotubes embedded in oriented polymeric nanofibers by electrospinning, Langmuir 20 (2004) 9852–9855.
[9] F. Samperi, M. Montaudo, C. Puglisi, Essential role of chain ends in the Ny6/PBT exchange. A combined NMR and MALDI approach, Macromolecules 36 (2003) 7143–7151.
[10] G. Tsagaropoulos, A. Eisenberg, Direct observation of two glass transitions in silica-filled polymers. Implications to the morphology of random ionomers, Macromolecules 28 (1995) 396–398.
[11] B. Fiedler, F.H. Gojny, M.H.G. Wichmann, M.C.M. Nolte, K. Schulte, Fundamental aspects of nano-reinforced composites, Composites Science and Technology 66 (2006) 3115–3125.
[12] M. Moniruzzaman, K.I. Winey, Polymer nanocomposites containing carbon nanotubes, Macromolecules 39 (2006) 5194–5205.
[13] J.N. Coleman, U. Khan, W.J. Blau, Y.K. Gun'ko, Small but strong: A review of the mechanical properties of carbon nanotube – polymer composites, Carbon 44 (2006) 1624–1652.
[14] H.J. Yoo, K.H. Kim, S.K. Yadav, J.W. Cho, Effects of carbon nanotube functionalization and annealing on crystallization and mechanical properties of melt-spun carbon nanotubes/poly(ethylene terephthalate) fibers, Composites Science and Technology 72 (2012) 1834–1840.
[15] O. Breuer, U. Sundararaj, Big returns from small fibers: a review of polymer/carbon nanotube composites, Polymer Composites 25 (2004) 630–645.
[16] Z. Li, G. Luo, F. Wei, Y. Huang, Microstructure of carbon nanotubes/PET conductive composites fibers and their properties, Composites Science and Technology 66 (2006) 1022–1029.
[17] D. Xu, Z. Wang, Role of multi-wall carbon nanotube network in composites to crystallization of isotactic polypropylene matrix, Polymer 49 (2008) 330–338.
[18] S. Yesil, G. Bayram., Poly(ethylene terephthalate)/carbon nanotube composites prepared with chemically treated carbon nantubes, Polymer Engineering Science 51 (2011) 1286–1300.
[19] J.Y. Kim, H.J. Choi, C.S. Kang, S.H. Kim, Influence of modified carbon nanotube on physical properties and crystallization behavior of poly(ethyelene terephthalate) nanocomposites, Polymer Composties 31 (2010) 858–869.
[20] P. Ajayan, J.M. Tour, Materials science: nanotube composites, Nature 447 (2007) 1066–1068.
[21] X.L. Xie, Y.W. Mai, X.P. Zhou, Dispersion and alignment of carbon nanotubes in polymer matrix: a review, Materials Science Engineering R 49 (2005) 89–112.
[22] A. Hirsch, Functionalization of single-walled carbon nanotubes, Angiewandte Chemical International Edition 41 (2002) 1853–1859.
[23] A. Garg, S.B. Sinnott, Effect of chemical functionalization on the mechanical properties of carbon nanotubes, Chemical Physics Letters 295 (1998) 273–278.
[24] A.H. Barber, S.R. Cohen, H.D. Wagner, Measurement of carbon nanotube – polymer interfacial strength, Applied Physics Letters 82 (2003) 4140–4142.
[25] M.J. O'Connell, P. Boul, L.M. Ericson, C. Huffman, Y.H. Wang, E. Haroz, Reversible water-solubilization of single-walled carbon nanotubes by polymer wrapping, Chemical Physics Letters 342 (2001) 265–271.
[26] J. Chen, H.Y. Liu, W.A. Weimer, M.D. Halls, D.H. Waldeck, G.C. Walker, Noncovalent engineering of carbon nanotube surfaces by rigid, functional conjugated polymers, Journal of American Chemical Society 124 (2002) 9034–9035.
[27] X. Yang, Q. Li, Z. Chen, H. Han, Fabrication and thermal stability studies of polyamide 66 containing triaryl phosphine oxide, Bulletin of Materials Science 32 (2009) 375–380.
[28] J.E. McGrath, Ring-opening Polymerization, American Chemical Society, Washington, DC7.
[29] R. Nirmala, K.T. Nam, S.J. Park, Y.S. Shin, R. Navamathavan, H.Y. Kim, Formation of high aspect ratio polyamide-6 nanofibers via electrically induced double layer during electrospinning, Applied Surface Science 256 (2010) 6318–6323.
[30] L. Li, C.Y. Li, C. Ni, L. Rong, B. Hsiao, Structure and crystallization behavior of Nylon 66/multi-walled carbon nanotube nanocomposites at low carbon nanotube contents, Polymer 48 (2007) 3452–3460.
[31] B.P. Singh, D. Singh, R.B. Mathur, T.L. Dhami, Influence of surface modified MWCNTs on the mechanical, electrical and thermal properties of polyimide nanocomposites, Nanoscale Research Letters 3 (2008) 444–453.
[32] Y. Gao, Z. Wang, R. Wang, J. Liang, L. Wang, Preparation and characterization of MWCNTs/E44, Journal of Materials Science and Technology 22 (2006) 117–122.
[33] K.T. Kim, W.H. Jo, Non-destructive functionalization of multi-walled carbon nanotubes with naphthalene-containing polymer for high performance Nylon66/multi-walled carbon nanotube composites, Carbon 49 (2011) 819–826.
[34] Z. Shang, S. Huang, X. Xu, J. Chen, Mo/MgO from avalanche-like reduction of $MgMoO_4$ for high efficient growth of multiwalled carbon nanotubes by chemical vapor deposition, Materials Chemistry and Physics 114 (2009) 173–178.
[35] B. Zhao, L. Zhang, X. Wang, J. Yang, Surface functionalization of vertically-aligned carbon nanotube forests by radio-frequency Ar/O_2 plasma, Carbon 50 (2012) 2710–2716.
[36] K. Yang, M. Gu, Y. Guo, X. Pan, G. Mu, Effects of carbon nanotube functionalization on the mechanical and thermal properties of epoxy composites, Carbon 47 (2009) 1723–1737.
[37] R. Sengupta, S. Sabharwal, A.K. Bhowmick, T.K. Chaki, Thermogravimetric studies on Polyamide-6,6 modified by electron beam irradiation and by nanofillers, Polymer Degradation and Stability 91 (2006) 1311–1318.
[38] H. Mitomo, K. Nakazato, I. Kuriyama, Lamellar thickening behavior of nylon-6,6 crystal by annealing, Polymer 19 (1978) 1427–1432.
[39] W.G. Weng, G.H. Chen, D.J. Wu, Crystallization kinetics and melting behavior of nylon6/foliated graphite nanocomposites, Polymer 44 (2003) 8119–8124.
[40] M.Y. Liu, Q.W. Zhao, Y. Wang, C.G. Zhang, Z.S. Mo, S.K. Cao, Melting behaviors, isothermal and non-isothermal crystallization kinetics of nyon1212, Polymer 44 (2003) 2537–2545.
[41] G.S. Zhang, D.Y. Yan, Crystallization kinetics and melting behavior of nylon 10, 10 in nylon 10,10 – montmorillonite nanocomposites, Journal of Applied Polymer Science 88 (2003) 2181–2188.
[42] Y.J. Li, X.Y. Zhu, G.H. Tian, D.Y. Yan, E.L. Zhou, Multiple melting endotherms in melt-crystallized nylon 10,12, Polymer International 50 (2001) 677–682.
[43] L. Li, C.Y. Li, C. Ni, L. Rong, H. Hsiao, Structure and crystallization behavior of Nylon 66/multi-walled carbon nanotube nanocomposites at low carbon nanotube contents, Polymer 48 (2007) 3452–3460.
[44] J.P. Bell, P.E. Slade, J.H. Dumbleton, Multiple melting in nylon 66, Journal of Polymer Science A 2 (1968) 1773–1781.